CHALMERS
UNIVERSITY OF TECHNOLOGY

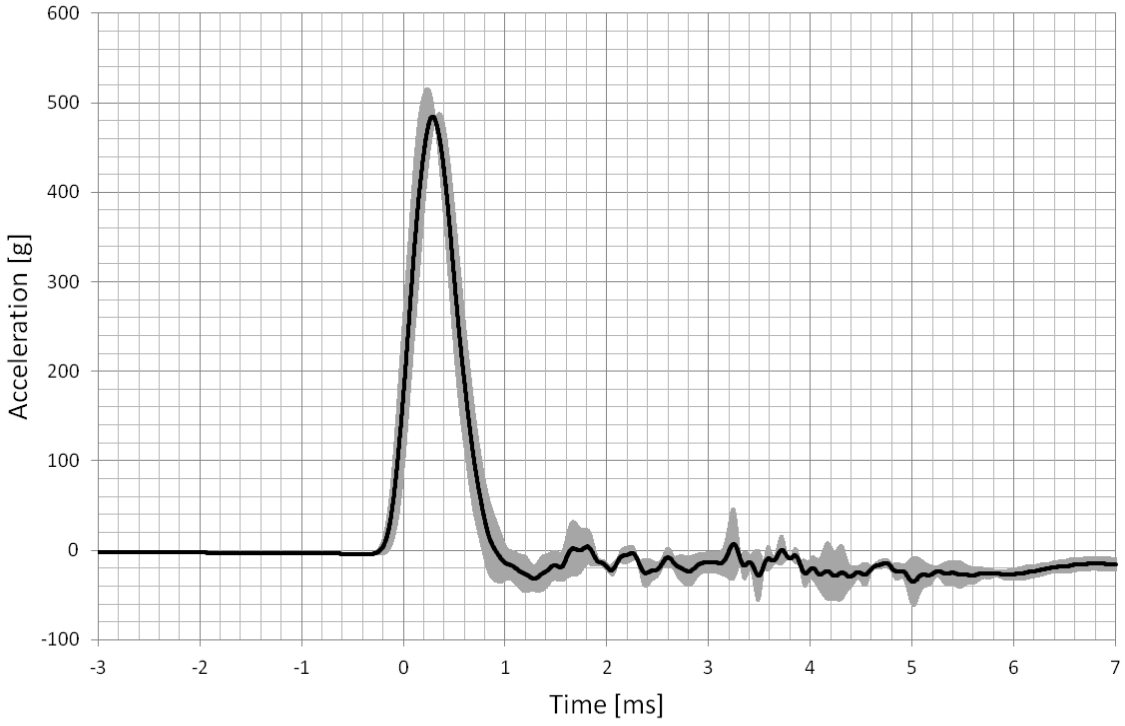

Shock-test Evaluation of The Audiometric Bone Vibrator Radioear B71

SOLOMON AMBISSA TEREFE

Department of *Signal and Systems*

CHALMERS UNIVERSITY OF TECHNOLOGY

Gothenburg, Sweden 2014

EX040/2014

Abstract

A bone vibrator is an electro-mechanical device that is used in the field of diagnostic audiology to assess the degree of sensorineural hearing loss. This device is likely to be exposed to mechanical impact from rough handling or accidental drops when it is used in clinics. Its robustness is therefore important to investigate in order to find out if it has any effect on its electro-acoustic performance. The most commonly used bone vibrator is the Radioear B71, which has never been tested for mechanical impact and a new bone vibrator from Interacoustics is soon available on the market under the trade name Radioear B81. The aim of this thesis work was to develop a methodology of how to investigate the robustness of bone vibrators that later can be applied to B71 and B81 in a comparative study. First, a literature study was made and then a drop-test setup based on the pendulum principle that can exert mechanical acceleration pulses to the bone vibrators was constructed. It is recommended in the standard IEC 60068-2-27 to apply a half-sine pulse shape of peak acceleration 500 g over 1 ms for structural integrity tests on micro-assemblies. The measurement setup was then tested on one B71 by measuring its electro-acoustic performance before and after exposure to different shock levels in different directions. The electro-acoustic performance was evaluated by measuring the frequency response and total harmonic distortion (THD). A major change in the electro-acoustic performance was first observed at 1500 g over 0.5 ms, with a maximum loss in magnitude of 5.2 dB in the frequency response at 10 kHz. All six directions were then tested for 1500, 2000 and 3000 g, which gave a maximum loss of 9.7 dB at 5625 Hz and in average 4 dB with a standard deviation of 1.2 dB for all frequencies between 100 and 10000 Hz. As the magnitude of the frequency response decreased, so did the THD with maximum 32.5 % at 150 Hz and in average 4.9 ± 8.5 %. The effects of mechanical shocks applied to B71 are reduced gain and THD.

Keywords: B71, B81, drop-test, electro-acoustics

Acknowledgements

First and foremost, I would like to express my deepest appreciation to my supervisor Karl-Johan Fredén Jansson for his unprecedented help and support throughout the thesis work. I am really thankful that he was more like a thesis mate and a friend. I want to extend my gratitude to my examiner Bo Håkansson for giving me the chance to work on this thesis. I also want to thank Hamidreza Taghavi for the great coffee break discussions and for his knowledgeable ideas. In addition, I would like to thank Swedac Acoustic AB for their kind cooperation and for sharing their state of the art expertise in the area of vibration damping. I am indebted to my families and to many of my friends and I would like to use this chance express my gratitude for them as well. Last but not least, I would like to thank my fiancé Fozia Ahmed for her invaluable support throughout the years.

Contents

1. Introduction

In the field of audiometry, air conduction (AC) and bone conduction (BC) hearing is investigated together. In the AC audiometry, speakers or earphones are used to deliver different sound pressure levels to the outer ear and in the BC audiometry, a bone vibrator is used to stimulate the inner ear (cochlea) by creating vibrations in the skull bone. The results of the patient's ability to hear the AC and BC sound is then compared in an audiogram. The bone vibrator is either attached to the patient's forehead or to the mastoid portion of the temporal bone behind the ear pinna. The most extensively used bone vibrator has been the Radioear B71 since the 1970's. It is a relatively small device with low weight and it can give high output levels over a wide range of frequencies. However it has some well-known limitations at low frequencies where the total harmonic distortion (THD) is high. Recently, a new bone vibrator from Interacoustics was developed under the trade name Radioear B81. It has improved performance at low frequencies compared to B71 and is compatible with same audiometer types (Fredén Jansson KJ et al. (2014)).

Quality testing of mobile electronic products that are prone to mechanical impact is an integral part of the production process (Harpreet S. Dhiman, Xuejun Fan, Tiao Zhou, 2008). The effect of mechanical impact due to accidental drops when used in clinical setting has never been scientifically investigated for both B71 and B81 bone vibrator types. A study of the electro-acoustic performance of these devices after undergoing drops from varying heights would thus be helpful in optimizing the devices. This kind of test indicates if a dropped device requires a recalibration in the audiometer in order to generate the correct hearing levels for all frequencies.

In this thesis, the design of drop-test reliability assessment equipment is presented. This has subsequently been used to impart drop shocks of different intensities to B71. In particular, the electro-acoustic performance of the B71 was investigated after being subjected to drops shocks of increasing severity. The electro-acoustic performance in this context means frequency response and THD.

2. Theory

2.1 Hearing impairments and Audiometry

Hearing impairment can be due to several factors. These can be aging, genetic, noise exposure, chemical exposure or physical trauma. A hearing loss can be classified in to three main types: conductive loss, sensorineural loss and the combination of the two called mixed hearing loss (Hearing Loss Association of America, 2005).

Conductive hearing loss is the inability of sound to reach the inner ear. This can be due to defects with the auditory canal and ear drum or malfunctions of the ossicles in the middle ear. Rehabilitation to this kind of hearing loss can be achieved by either surgically removing the obstruction present on the auditory pathway or using a middle ear hearing implant. Sensorineural hearing loss arises due to a dysfunction in the inner ear, which means the cochlea or the nerve that relays the impulse to the brain or damage in the brain. This kind of hearing loss is rarely treated by medicine or surgery (Hearing Loss Association of America, 2005). A more common treatment is to use conventional air conduction hearing aids to amplify the sound transmitted through the ear canal and in certain cases it can be corrected by a cochlear implant.

Diagnosis of a patient with a suspected hearing loss is performed by an Audiologist. The audiologist performs both AC and BC hearing tests to assess the hearing loss. The results of hearing thresholds tests are plotted on an audiogram. The audiogram shows AC thresholds for various tested frequencies in relative to the audiometric zero, see Fig.1. Audiometric zero is a standard indicating the hearing threshold level of an otologically normal person (IEC. 60645-1). Calibration of AC levels can be performed by artificial ear (specified IEC 60318-1) or acoustic reference coupler (specified IEC 60318-3) whereas calibration of BC levels is performed using an artificial mastoid and reference equivalent threshold force levels (RETFLs) specified in ISO 389-3. Prior to investigation, any audiometer should be calibrated to ensure the stimulus received by the patient is in fact the reading displayed by the audiometer.

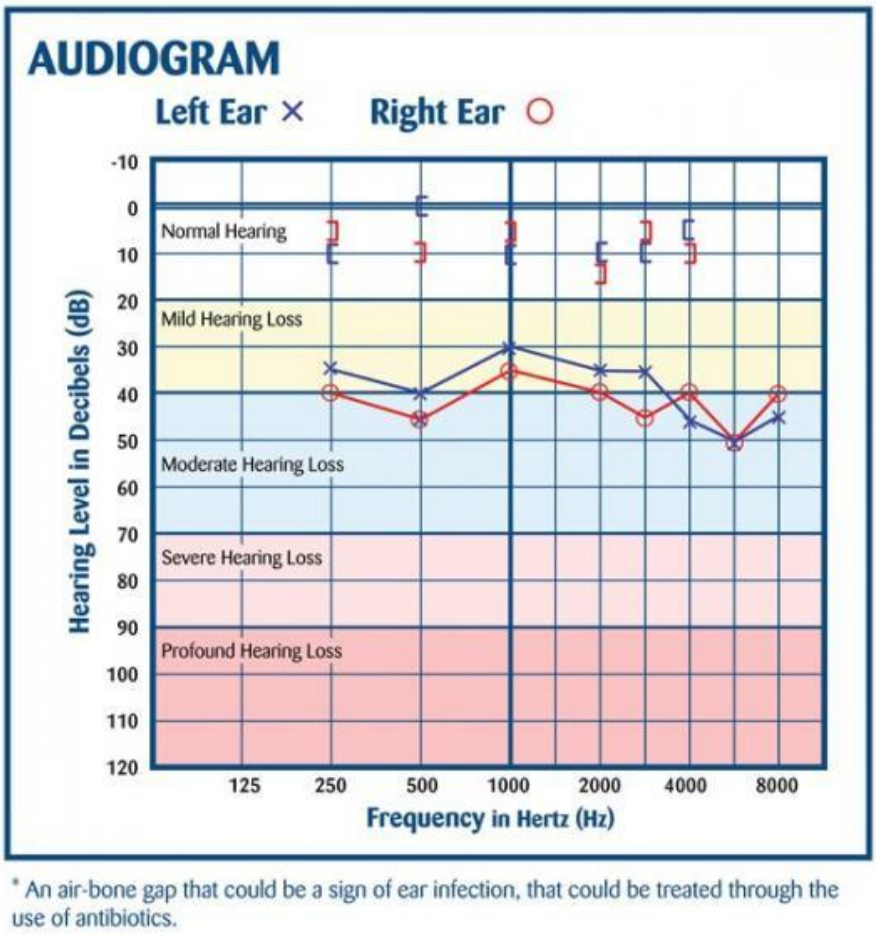

Figure 1. An Audiogram showing BC and AC thresholds. The square brackets shown on the top are BC thresholds [for right ear and] for left ear. X and O shows AC thresholds for the left and right ear, respectively.(Image taken from : http://www.terracehearing.com).

2.2 Radioear B71

The interest in bone conduction since it was described in 19th century was its usefulness as a diagnostic tool. In recent years bone conduction has gained popularity in the use of hearing aids such as the Bone Conduction Implant (BCI) and Bone Anchored hearing Aid (BAHA) (Eeg-Olofsson et al. (2014) and Tjellström et al. (2001)). Evolvement towards fancier applications like in the Google glasses where it is employed to relay information to a user by a bone conduction transducer in the frames is one interesting and recent advancement outside healthcare.

Transducers for bone conduction can be constructed based on different technologies such as electrodynamic, piezoelectric or magnetostrictive. The electrodynamic transducers of the variable reluctance type such as the transducer in B71 are most commonly used transducer types in hearing aid applications due to their ability to achieve high force levels over a wide frequency range and their small size. These types of transducers operate based on the horseshoe magnet principle where a time varying magnetic flux in a closed magnetic circuit forces a small air gap to open and close accordingly. The parts inside the transducer comprise a permanent magnet, spring suspension, two coils, an iron bobbin and yoke material. Static flux is created due to the permanent magnet and dynamic flux due to time-varying current in the two coils. The spring suspension maintains the air gap between the armature and the yoke so it does not collapse.

The external view of the B71 bone vibrator and a cross-sectional sketch of its transducer are shown in Fig. 2. It has a plastic housing with a circular attachment surface area of 1.75- cm^2. A steel spring headband is used in the clinic to press the bone vibrator to the mastoid area behind the ear to keep it in place during the hearing investigation.

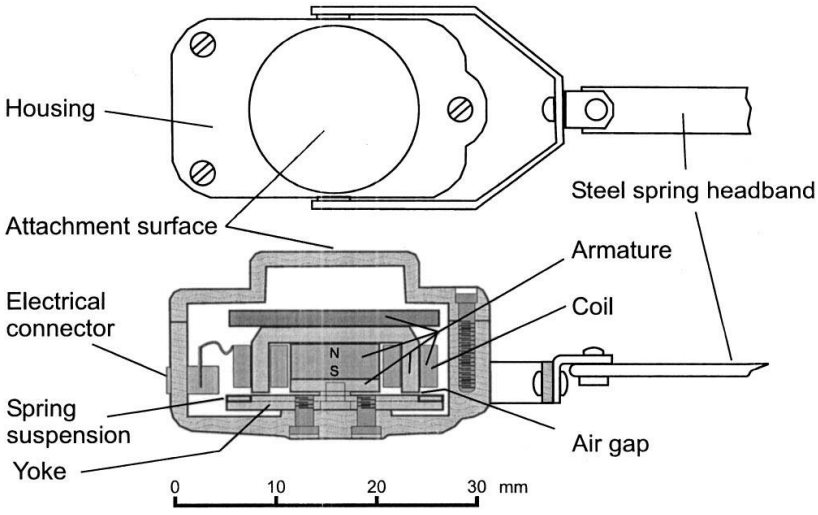

Figure 2. The housing of B71 and a cross-sectional view of its transducer (Image taken from Håkansson 2003).

The magnetic flux directions inside the B71 transducer and the flux-force relation is shown in Fig. 3. The total force produced by the transducer is approximately proportional to the total magnetic flux in the air gap, which comprises both the static and time-varying fluxes. Moreover,

$$F_{tot} \propto (\phi_0 + \phi_\sim)^2 = {\phi_0}^2 + 2\phi_\sim\phi_0 + \phi_\sim, \qquad (1)$$

where ϕ_0 is the static flux from the permanent magnet and $\phi_\sim$ is the dynamic flux generated by the coils. The relation in equation (1) is non-linear and hence will generate non-linear distortion. To avoid this, the static magnetic flux has to be much higher than the dynamic magnetic flux, i.e. $\phi_0 \gg \phi_\sim$. However, an increase in ϕ_0 increases the static force which means the force on the spring increases, requiring a stiffer spring in order for the air gap not to collapse.

A mechanical interaction between the suspension spring compliance *C*, and a counteracting mass *m* that partly consists of the armature, yoke, coil, magnet and an additional mass, see Fig. 3, will create a resonance frequency in the frequency response of B71 given by:

$$f_r \approx \frac{1}{2\pi\sqrt{mC}} \qquad (2)$$

Ordinarily, audiometric transducers requires the resonance frequency to be low, but higher than the lowest frequency of interest between 250-500 Hz in BC audiometry. However, it is evident from equation (2) that in order to have a lower f_r for a given compliance *C*, the counteracting mass should be increased which is not desirable since this increases the total weight and size of the transducer.

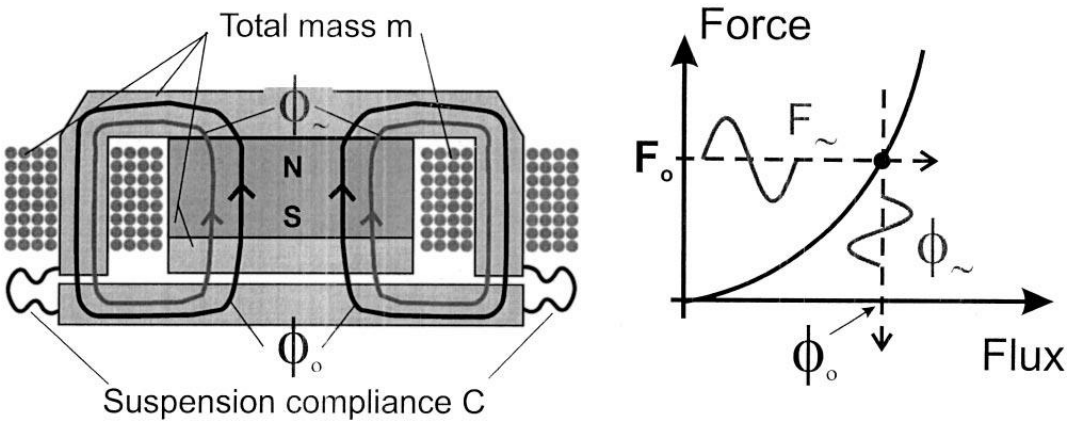

Figure 3. The magnetic flux direction inside the B71 and the flux to force characteristics, described by equation (1) (Image taken from Håkansson 2003).

2.3 Radioear B81

To overcome the shortcomings of conventional variable reluctance type transducers mentioned in the previous section, the balanced electromagnetic separation transducer (BEST) was designed by Håkansson (2003). This design has recently been adapted for serial production by Ortofon in the motor unit of the new Radioear B81 from Interacoustics. The cross sectional view of the BEST transducer, showing its magnetic circuitry is shown in Fig. 4. It uses four permanent magnets and four corresponding air gaps to achieve a force balance, in comparison with the variable reluctance transducer where only one permanent magnet is used.

The total vibrating force of the BEST transducer can be approximated by subtracting the force in the upper air gap F_{Upper} from the force in the lower gap F_{Lower} .

$$F_{Lower} \propto \left(\frac{\phi_0}{2} + \phi_{\sim}\right)^2 = \left(\frac{{\phi_0}^2}{4} + \phi_{\sim}.\phi_0 + {\phi_{\sim}}^2\right) \quad (3)$$

$$F_{Upper} \propto \left(\frac{\phi_0}{2} - \phi_{\sim}\right)^2 = \left(\frac{{\phi_0}^2}{4} - \phi_{\sim}.\phi_0 + {\phi_{\sim}}^2\right) \quad (4)$$

$$F_{tot} = F_{Lower} - F_{Upper} \propto 2\phi_0\phi_{\sim}. \quad (5)$$

In Equation (5), nonlinearities and static forces are canceled out and this makes the BEST transducer more linear than the variable reluctance type transducers.

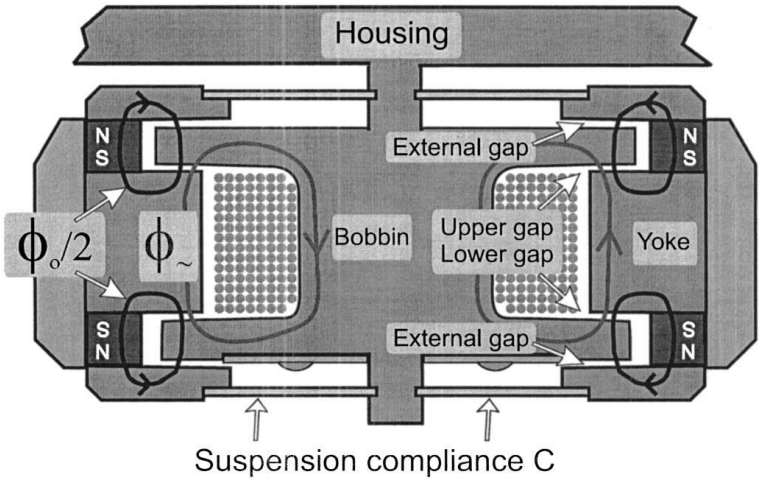

Figure 4. Cross-sectional view of the BEST transducer used in the B81 (Image taken from Håkansson 2003).

The external view of both bone vibrators are shown in Fig. 5, together with the corresponding dimensions. The weight of B71 and B81 is 19.9 and 20 g respectively.

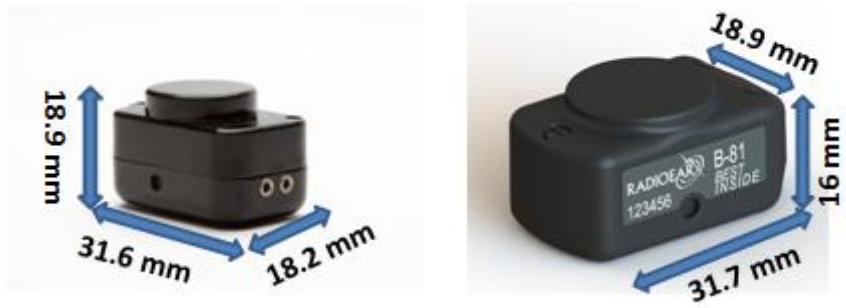

Figure 5. External view of B71 (left) and B81 (right).

2.4 Electro-acoustic performance of B71 and B81

The differences in the electro-acoustic performance brought by the previously mentioned transducer design differences is seen in the measurement of THD and maximum hearing level of B71 and B81. Fig. 6 and Fig. 7 shows the mean value of the THD for six of each vibrator types, measured by Fredén Jansson KJ et al. (2014). As can be seen, B71 has high harmonic distortion at low frequencies (100-1000 Hz). The maximum difference in THD for audiometric frequencies occurs at 250 Hz where B81 has THD of 1.88% and B71 has 28.06%. In addition, B71 has a maximum hearing level output 15 dB less than the minimum requirement for hearing level put forward by IEC 60645-1 at 250 Hz. However, the B81 fulfills the specification on the whole range of audiometric frequencies, shown in Fig. 7.

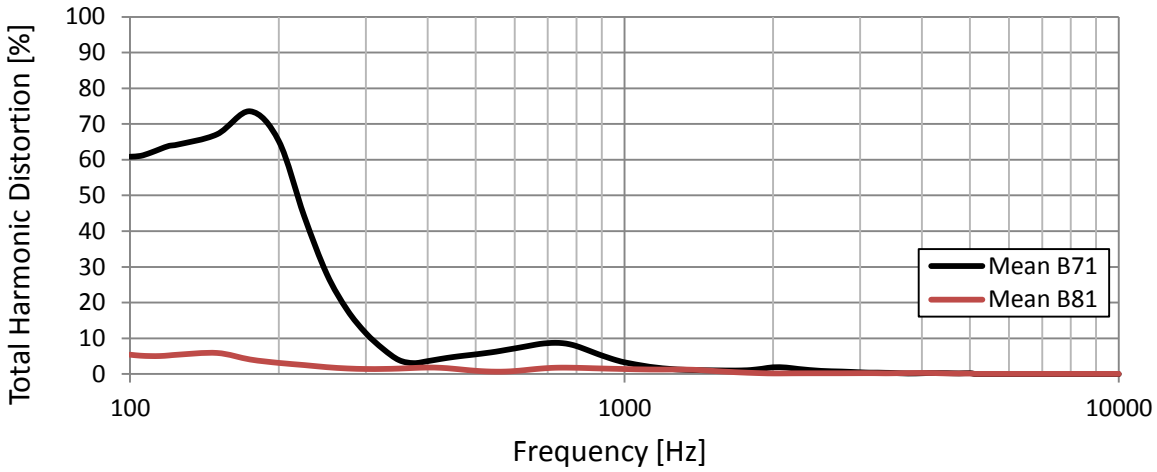

Figure 6. Mean value of THD for six B71s and six B81s.

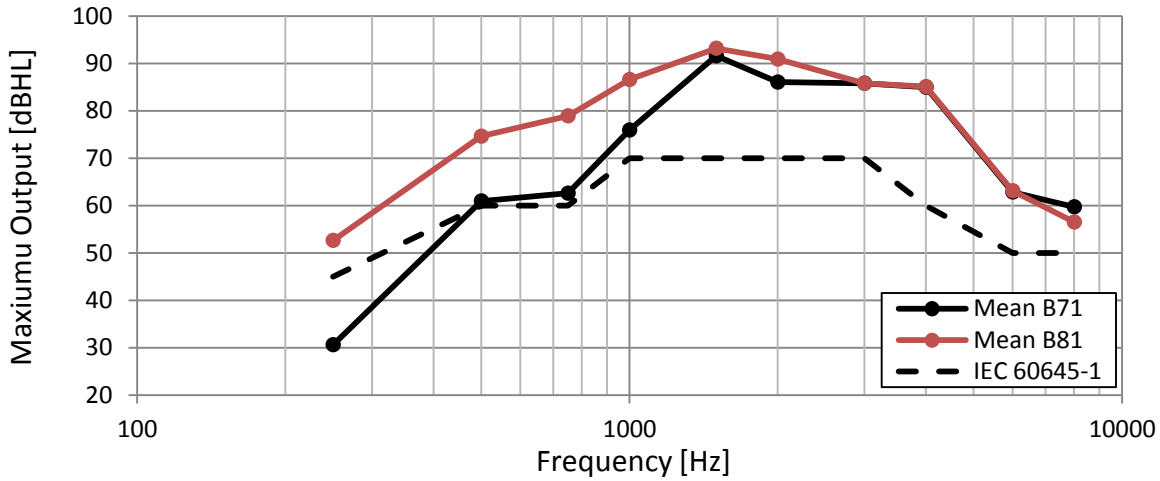

Figure 7. Mean value of maximum hearing level for six B71s and B81s.

2.5 Drop-test

Of all potential mechanical impacts, drop-test of handheld mobile devices that are prone to be dropped during their usable lifetime has become increasingly important. Until the 1990's, companies internally devised their own methods to assess the drop-test reliability of their own products. However, around the turn of the century initiatives were made to standardize the methods used in drop-testing. As a result, drop reliability assessment procedures on electrotechnical equipment were published by IEC, JEDEC, ETSI and ASTM standards (T. T. Mattila, L. Vajavaara, and J. Hokka, 2013). The formation of these standards provides important guide line to unify methodologies of drop reliability assessment.

Conventional drop-test equipment utilize the same principle as described by the JEDEC standard JESD22-B111 in which a guided horizontal platform with the taste specimen attached on the top is accelerated towards a strike surface (Boris Asdanin, 2009). This type of drop-tests are mostly constrained i.e. the specimen is not allowed to move naturally as it would in the real case. A realistic method for drop-testing was introduced by (Suresh Goyal and Edward K. Buratynski, 2000) to avoid this drawback. In the design the tested object is suspended with a string onto a drop-table, but it is released from the suspension just before the table strikes the ground allowing it to move freely thereafter.

The physical principle behind drop-test equipments is basically the same. The object being tested is released from a specified height to a strike surface. The potential energy of the object due to its mass and height is converted to kinetic energy as the object accelerates towards the strike surface. During the moment of impact the object stops from its downward course and reverses its direction. This is the point where maximum acceleration of the object is attained and where the change in velocity is the highest. This can simply be described by:

$$a = \frac{\Delta V}{\Delta t} \tag{6}$$

Newton's laws of motion states that a larger mass requires more force to accelerate meaning that it takes longer time for it to rebound. Therefore, when two objects of different mass are dropped from the same height the lighter object attains higher acceleration values with shorter pulse width and vice versa for the heavier object. An output of an accelerometer attached to a solid object being dropped is often approximated of half sine and is shown in Fig. 8.

Half sine drop shock acceleration can be described as

$$a = a_{peak} \sin\left(\frac{\pi t}{\Delta t}\right), \quad for\ 0 < t < \frac{T}{2} \tag{7}$$

where, Δt is the pulse width, a_{peak} is the amplitude and $\frac{T}{2}$ is the half-period.

Integrating equation (7) and equating with the velocity from the energy at impact, the drop height H to attain a certain shock can be calculated to:

$$H = \left(\frac{2a_{peak}\Delta t}{2g\pi}\right)^2, \tag{8}$$

where g is the gravitational acceleration $\approx 9.81\ {}^{m}/_{s^2}$.

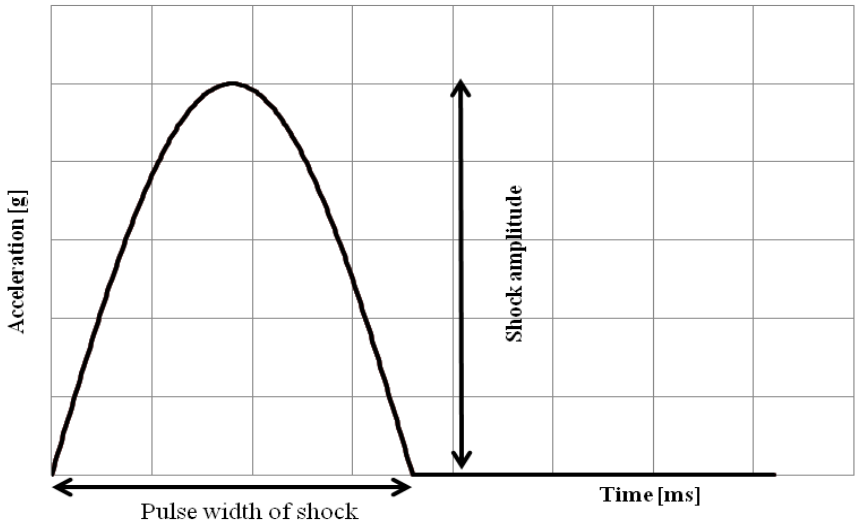

Figure 8. Half sine shock shape.

To consider the strike surface characteristics, a more realistic prediction model than described by equation (8) for the drop height needs to be derived. By assuming a solid object of mass M, and a strike surface being represented with spring stiffness K, the mass compresses the strike surface by a distance x during impact, see Fig. 9.

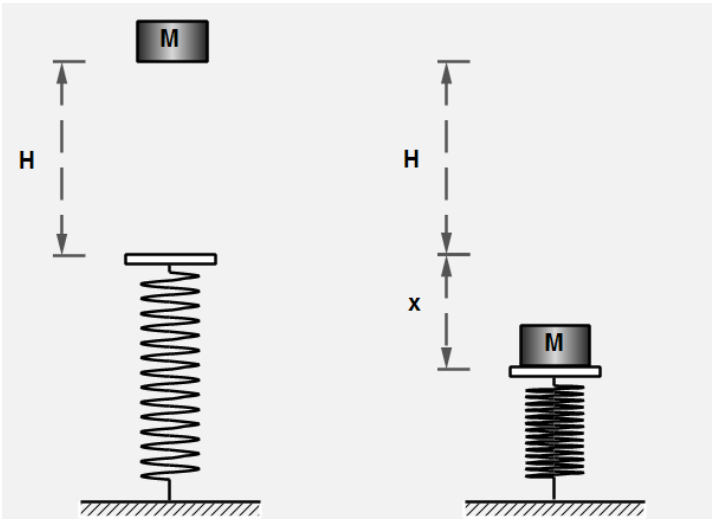

Figure 9. Model for drop height calculation assuming the strike surface as a spring. (Image taken from : http://www.okphysics.com).

The potential energy of the object due to its mass and the drop height will be stored in the spring when it's fully compressed. Moreover,

$$Mg(H + x) = \frac{Kx^2}{2}. \quad (9)$$

By applying Newton's and Hooke's law, the compression force is:

$$F = Ma_{peak} = -Kx. \quad (10)$$

Solving for the spring compression x from equation (10) gives

$$x = \frac{-Ma_{peak}}{K}. \quad (11)$$

The drop height is then found by substituting equation (11) into (9) so that

$$H = \left(\frac{M}{K}\right) \frac{{a_{peak}}^2 - 2ga_{peak}}{2g}. \quad (12)$$

This concludes the following statements:

- Acceleration is greater for stiffer strike surface and vise versa.
- An increase in drop height increases acceleration and vise versa.
- Greater acceleration levels will be attained for smaller mass objects and vise versa.

3. Methods and Equipments

3.1 Drop-test measurement setup

A pendulum arm shown in Fig. 10 was constructed as drop-test equipment. The arm is a rectangular rod with dimensions 40x40x1000 mm and is made of aluminum. In one end, it is attached to bearings that allow it to rotate with low friction. On the surface of the rod a vibration damping material by the name Isolermatta ISM 75 was adhered and the inside was also filled with a different vibration damping material. Both materials were provided by Swedac Acoustic AB.

Figure 10. The constructed drop-test equipment.

The idea at the beginning was for the bone vibrators to be attached in the opening at the free end of the aluminum rod. Unfortunately, too much vibration from the structure were picked up by the accelerometer B&K 4375 i.e. the amplitude were found to be higher than 20% of the main pulses amplitude (the minimum specified in IEC 60068-2-27:2008). After experimenting with a number of methods to remove the vibrations, a simple but convenient technique was devised. The solution was to attach the vibrators under test to a piece of aluminum plate separated from the rod by a damping sheet (Isolermatta ISM 75), protruding with a length of 0.17 m at the free end of the rod as shown in Fig. 11. An extra mass was added to the plate to make the overall weight greater than the weight of the vibrator. This mass helps to damp the vibration in the plate from the natural frequency of the bone vibrator. Minor high frequency vibrations that were present after the modification were removed by using a built in low-pass filter in the accompanying software for PicoScope 5203 PC oscilloscope, which was mainly used to display the acceleration pulse. A cut of frequency of the low-pass filter was set to 3 kHz with respect to not filter the main pulse signal information.

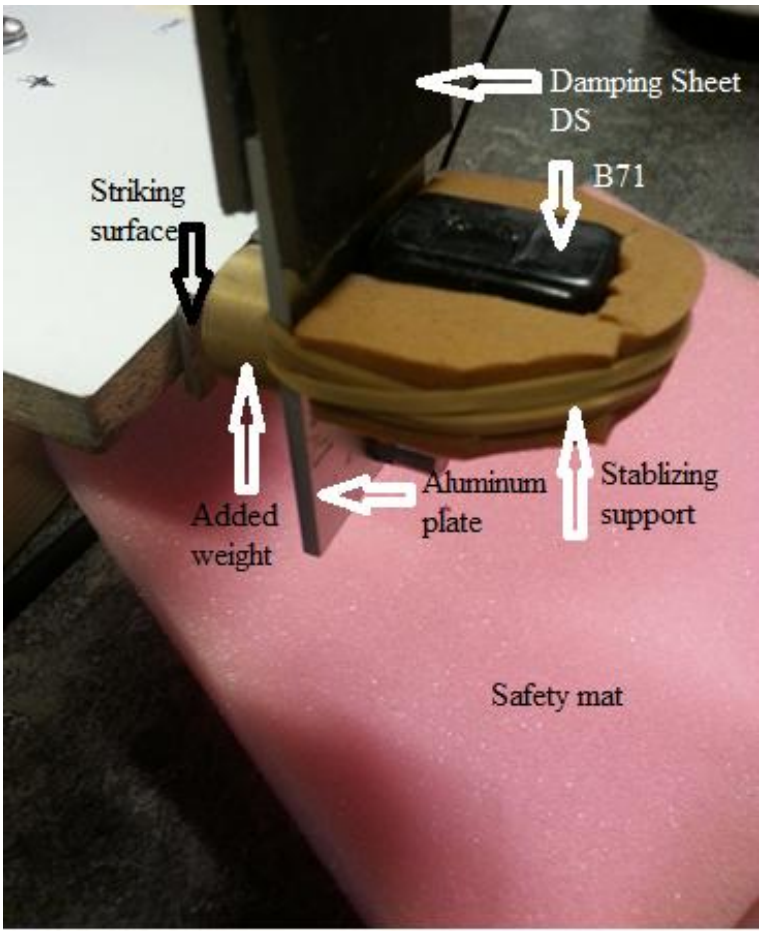

Figure 11. Attachment of the bone vibrator to the aluminum plate. The surface of the bone vibrator is assumed to receive the same acceleration severity as the aluminum plate.

The accelerometer B&K 4375 used in the measurement has the acceleration sensitivity $\alpha_1 = 3.11\ \mathrm{pC/g}$ and its output was fed to a charge amplifier B&K 2651 with the sensitivity of $\alpha_2 = 0.1\ \mathrm{mV/pC}$. The voltage pertaining to each acceleration levels was calculated using

$$V = \alpha_1 * \alpha_2 * Number\ of\ g \qquad (13)$$

and the voltage accelaretion dependence is plotted in Fig. 12.

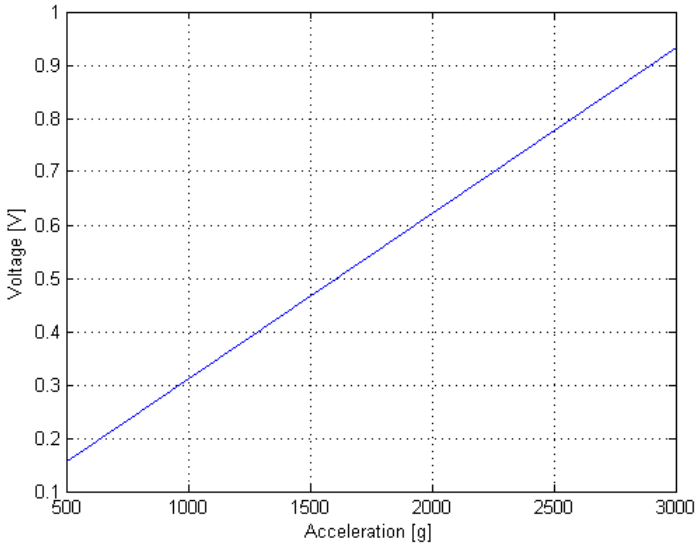

Figure 12. Relation of acceleretion to voltage level.

The drop height and hence the peak acceleration is varied depending on the rotating ends opening angle. The bearings can swing to a maximum opening angle of 180 degrees, which allows measurement to a maximum height of 2.34 m (two times the length of the rod and protruding damping sheet). A potentiometer was used to measure the opening angle and a B71 not used for drop-test was used to calibrate acceleration levels in g to the opening angle, at which the acceleration is attained, shown in Fig. 13.

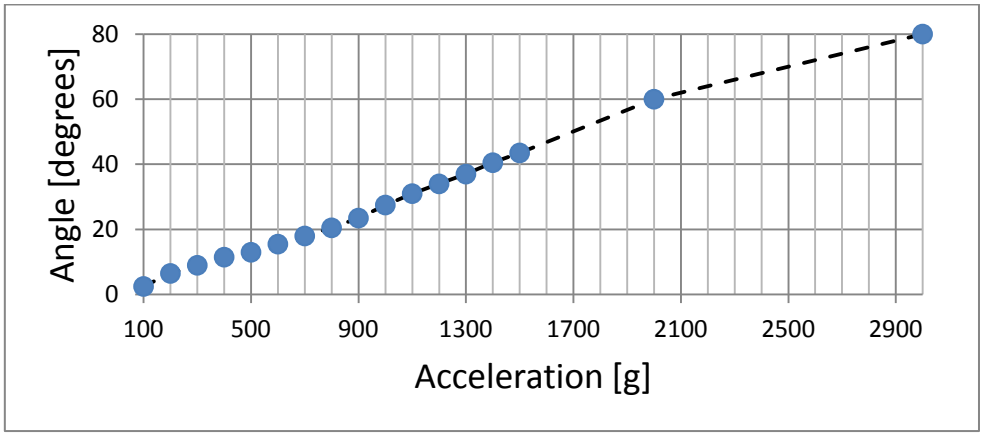

Figure 13. Relation of opening angle and acceleration.

The height that corresponds to each angle was calculated by equation (14) and the concept is demonstrated by Fig.14.

$$h = L - Lcos(-\theta_{max}) \qquad (14)$$

where h is the drop height, L is the pendulum length and θ_{max} is the opening angle.

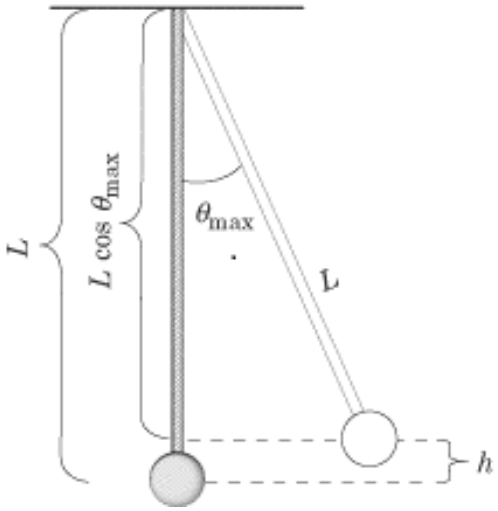

Figure 14. Drop height illustration. (Image taken from : http://www.sparknotes.com).

Finally, measurement of the initial performance of the B71 in terms of frequency response and THD were performed and a drop shock with increasing severity was applied to all six sides, as shown in Fig.15. To find a proper shock severity to measure from the severity of the shock was increased randomly from 500-3000 g. A significant change in the electro-acoustic performance was observed at 1500 g by a reduction in the frequency response amplitude at high frequencies.

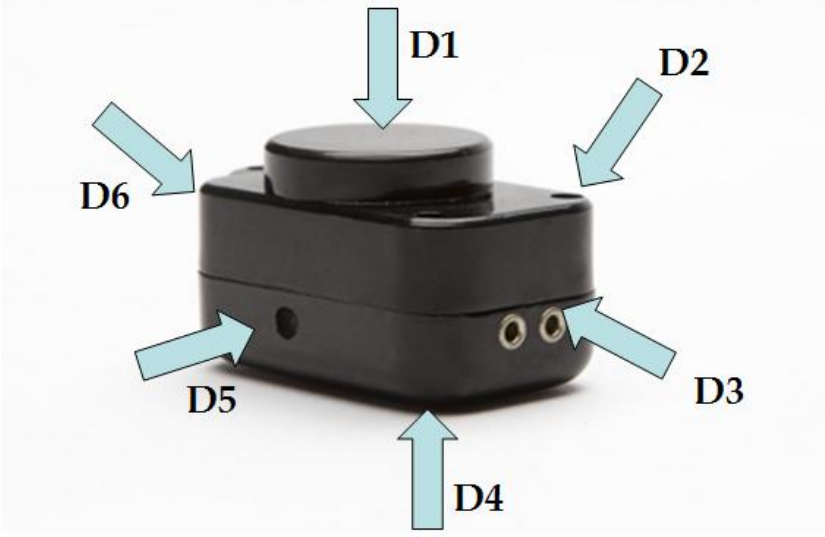

Figure 15. The six sides of the bone vibrator that were subjected to shocks.

3.2 Performance Measurement setup

The electro-acoustic measurement setup used in this thesis work is shown in Fig.16. The B71 bone vibretor was attached to a B&K 4930 artificial mastoid with a static force of 5.4 N. The signal was remotely generated by Agilent 33220A function/arbitrary wave form generator using Lab VIEW and amplified by LPA01 laboratory power amplifier. PicoScope 5203 PC Oscilloscope was used to measure the input voltage to the vibrator. The output from the artificial mastoid was fed to charge amplifier to avoid disturbance due to cable capacitance. In the end of the signal pathway, LabVIEW was used to collect the results of the measurement. Finally, Agilent 35670A FFT Dynamic Signal Analyzer was used to confirm the results of the measurement from the developed LabVIEW program.

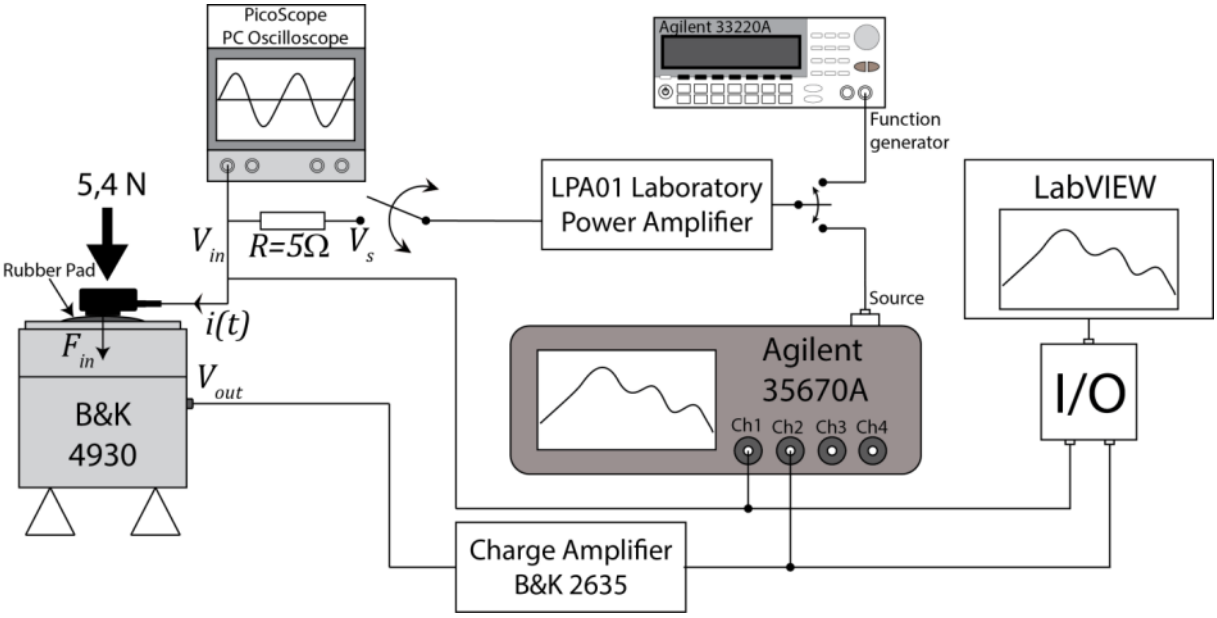

Figure. 16. Instrumentation for the measurement setup. The bone vibrator was attached to a B&K 4930 artificial mastoid with a force of 5.4 N, LPA01 laboratory amplifier was used to amplify the input signal to the bone vibrator. LabView was used to remotely control and read out the measurements (Image taken from Fredén Jansson KJ et al. (2014)).

The frequency response of the bone vibrator was measured as

$$G(j\omega) = \frac{V_{in}}{F_{in}} \quad (15)$$

from 100 - 10000 Hz and at $V_{in} = 1\, V_{RMS}$. The force F_{in} is the force on the rubber surface of the artificial mastoid. It was found by dividing V_{out} from the artificial mastoid by pad correction $P(j\omega)$ previously obtained by Fredén Jansson KJ et al. (2014).

The total harmonic distortion (THD) was calculated as (specified by IEC 60645-1).

$$THD = \sqrt{\frac{H_2^2 + H_3^2 + H_4^2 + \cdots + H_n^2}{H_1^2 + H_2^2 + H_3^2 + \cdots + H_n^2}}\ .100\%, \quad (16)$$

where H_n is the amplitude of the nth harmonic component in the RMS spectrum of the force F_{in}. THD was calculated using four harmonic components and the fundamental frequency for each audiometric frequency in the range 100 - 10000 Hz using an input voltage of $1V_{RMS}$.

4. Results and Discussion

4.1 Shock level of 500 g over 1 ms

The pulse for an acceleration of 500 g with duration of 1 ms is shown in Fig.17. The height at which the acceleration was attained is 3 cm. This shock level was applied to only three sides (D1, D2 and D3 in Fig. 15) of the vibretor. The other sides were skipped because there was no significant change in frequency response and THD.

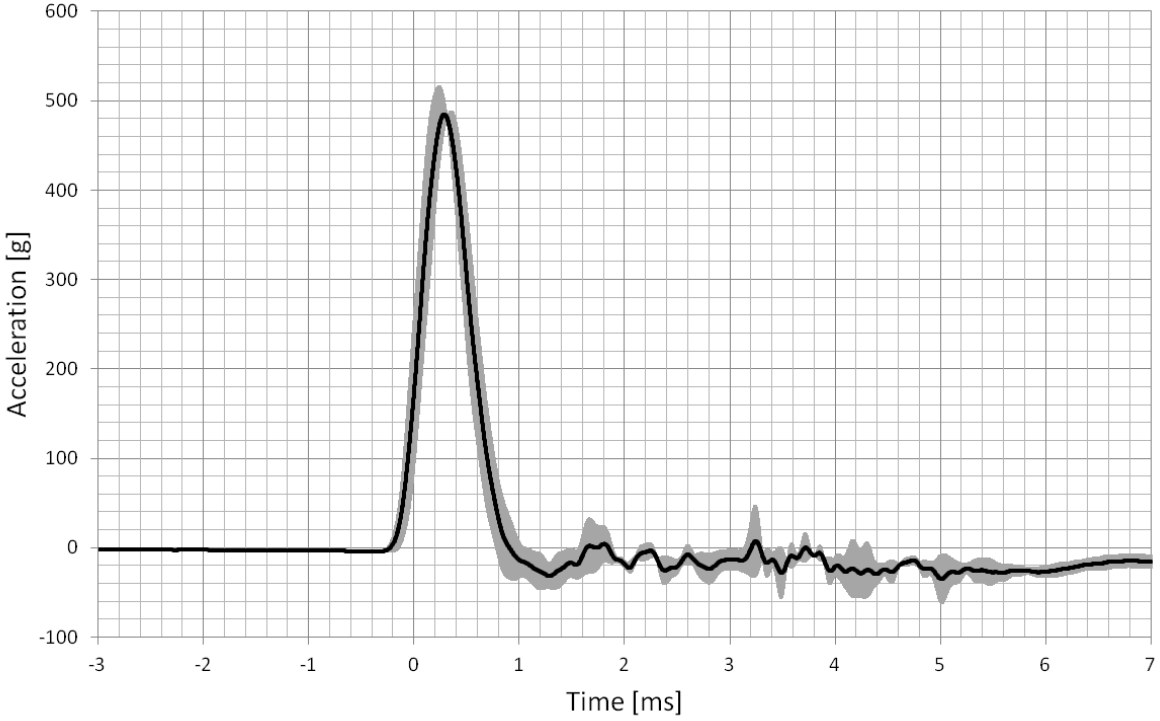

Figure 17. Acceleration pulse of 500 g over 1 ms imparted to the sides D1, D2 and D3. The average of the three pulses is shown in bold and the deviation from the average is shown in gray.

4.2 Shock level of 1500 g over 0.5 ms

Fig. 18, shows the pulse shape of 1500 g over a period of 0.5 ms. The drop height was 32 cm. All six sides of the bone vibrator were consecutively subjected to this shock level measuring the frequency response and THD after each instant. Both frequency response and the THD showed a major change at this shock level. A maximum loss of 5.2 dB occurred in the magnitude of the frequency response at 10000 Hz, see Fig. 19. The average loss in frequency response was 2.8 dB with a standard deviation of 1.6 dB. THD decreased in an average by 1.2 %, see Fig. 20.

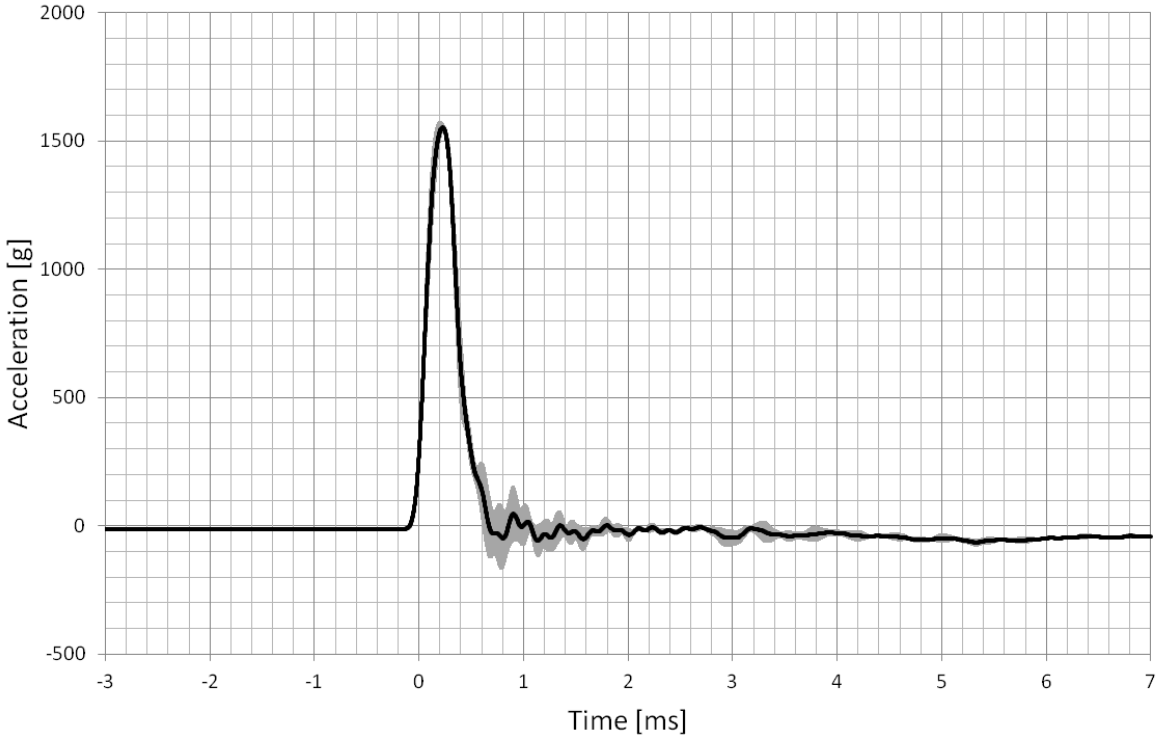

Figure 18. Shock pulse of 1500 g over 0.5 ms imparted to all sides of the bone vibrator, the average of the six pulses is shown in bold and the deviation from the average is shown in gray.

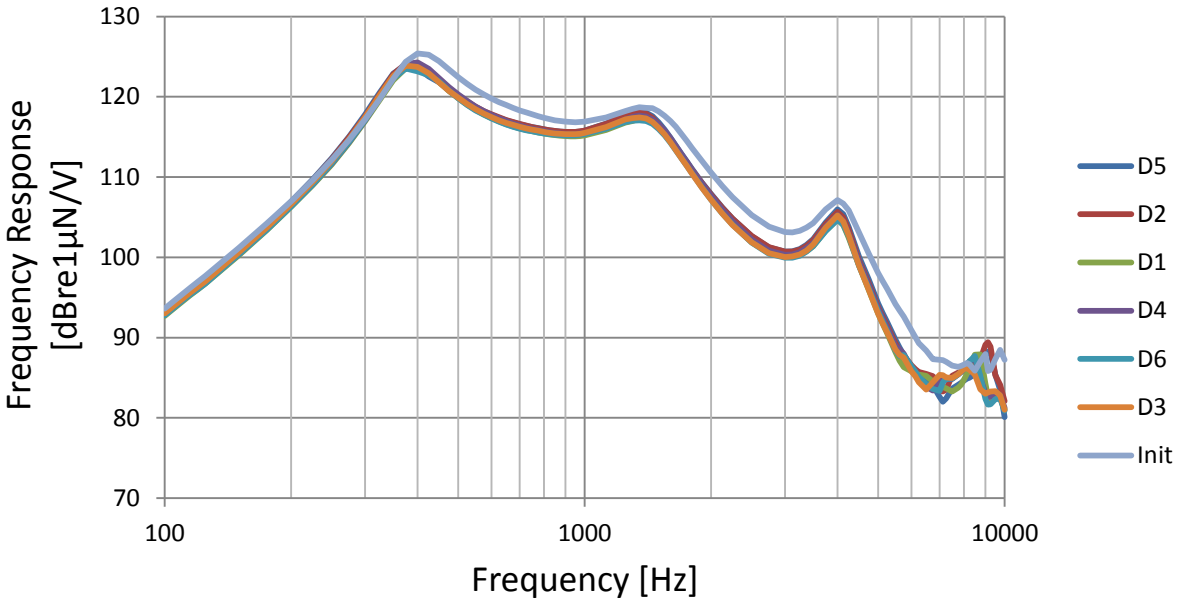

Figure 19. Frequency response of the bone vibrator after being subjected to a shock of 1500 g over the duration of 0.5 ms on all sides. Init on the legend indicate frequency response before shock.

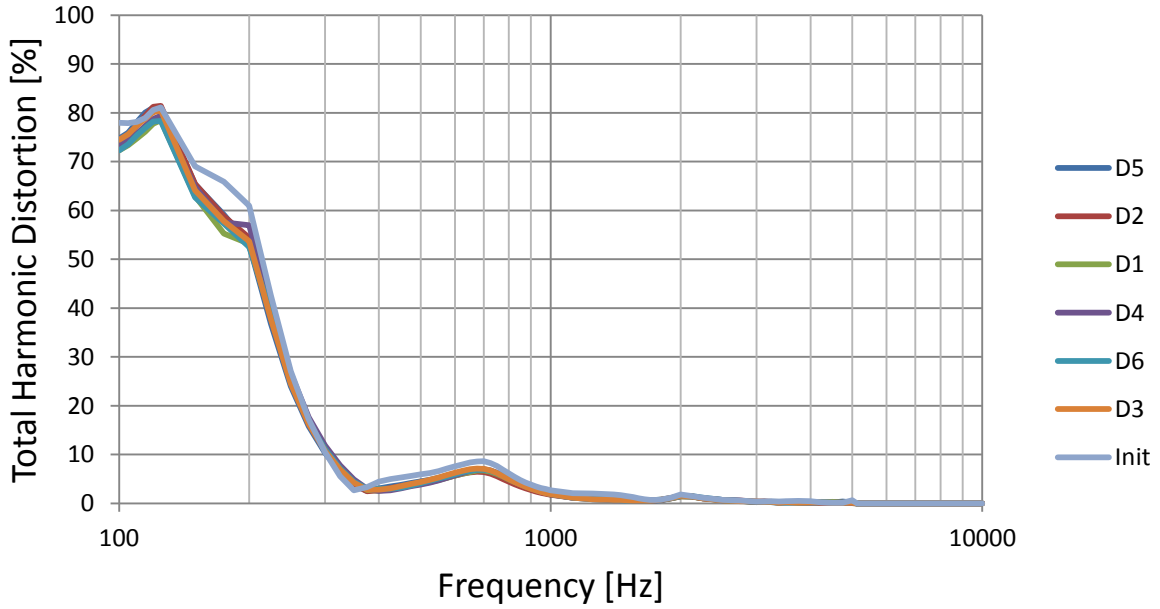

Figure 20. THD of the bone vibrator after being subjected to a shock of 1500 g over the duration of 0.5 ms on all side. Init on the legend indicate the THD before shock.

4.3 Shock level of 2000 g over 0.4 ms

A drop height of 53 cm gives a shock level of 2000 g with duration of 0.4 ms, see Fig. 21. Imparting this shock level to all sides of the bone vibretor resulted in a maximum loss of 8 dB at 10000 Hz and an overall average loss of 3.1 dB in the frequency response magnitude as shown in Fig. 22. As a result, there was an average decrease of 4.92% in THD, see Fig. 23.

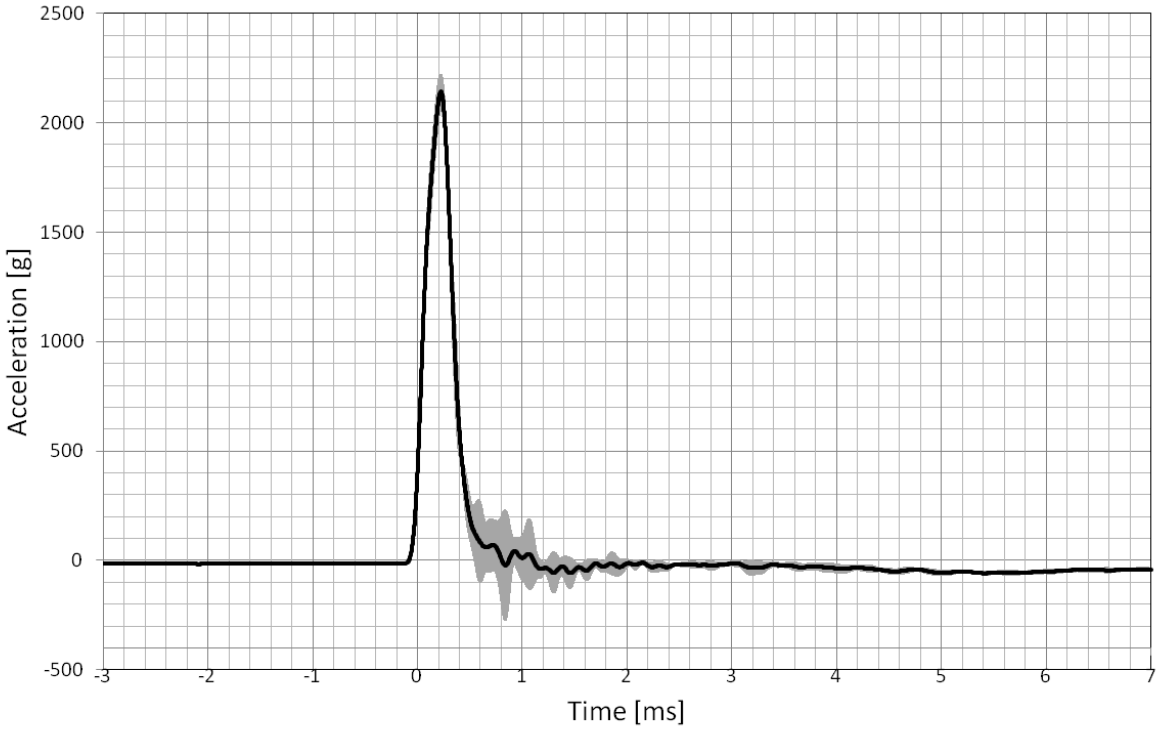

Figure 21. Shock pulse of 2000 g over 0.4 ms imparted to all sides of the bone vibrator, the average of the six pulses is shown in bold and the deviation from the average is shown in gray.

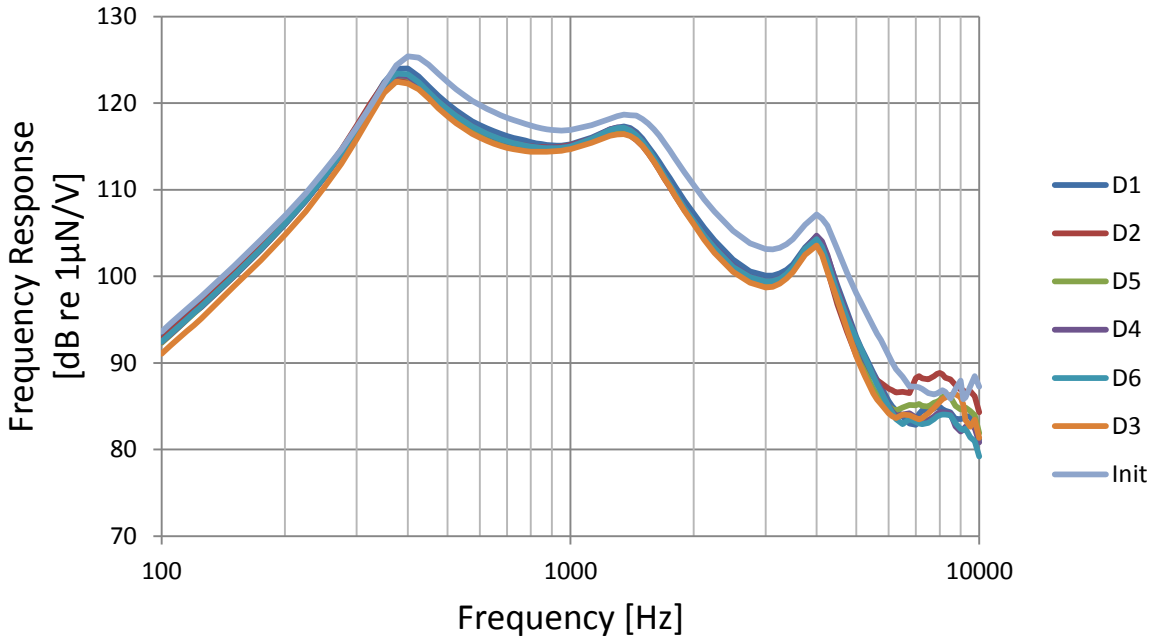

Figure 22. Frequency response of the bone vibrator after being subjected to a shock of 2000 g over the duration of 0.4 ms on all sides. Init on the legend indicate frequency response before shock.

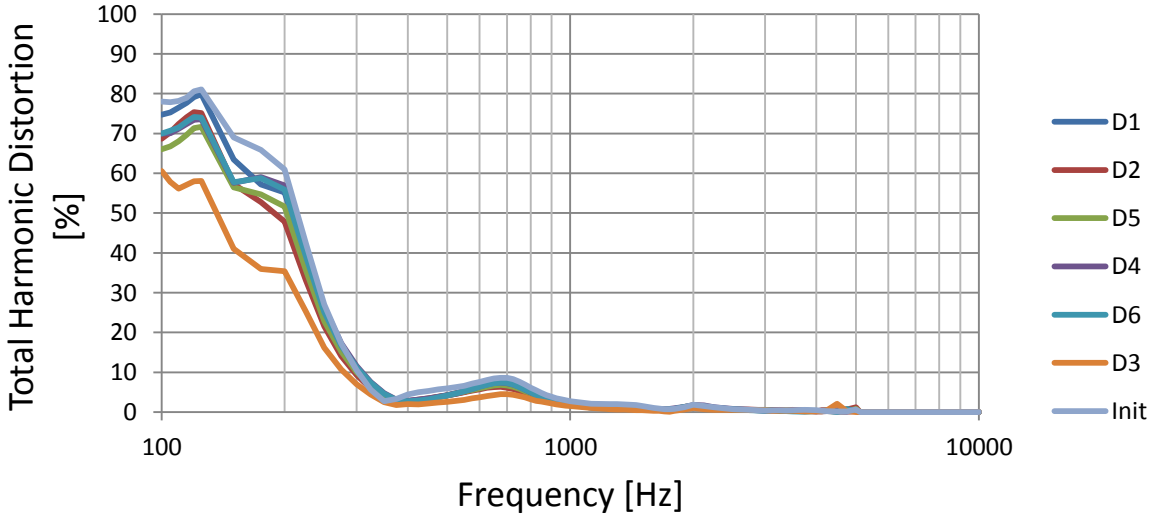

Figure 23.THD of the bone vibrator after being subjected to a shock of 2000 g over the duration of 0.4 ms on all sides. Init on the legend indicate the THD before shock.

4.4 Shock level of 3000 g over 0.3 ms

A shock pulse of 3000 g over 0.3 ms was achieved at a height 53 cm shown in Fig. 24. A maximum loss of 9.65 dB in the frequency response magnitude occurred at 5625 Hz and the average loss was 5.2 dB with a standard deviation of 1.8 dB, see Fig. 25. THD decreased in an average by 4.7 %, see Fig. 26. This average decrease in THD is less than the one obtained for shock level of 2000 g.

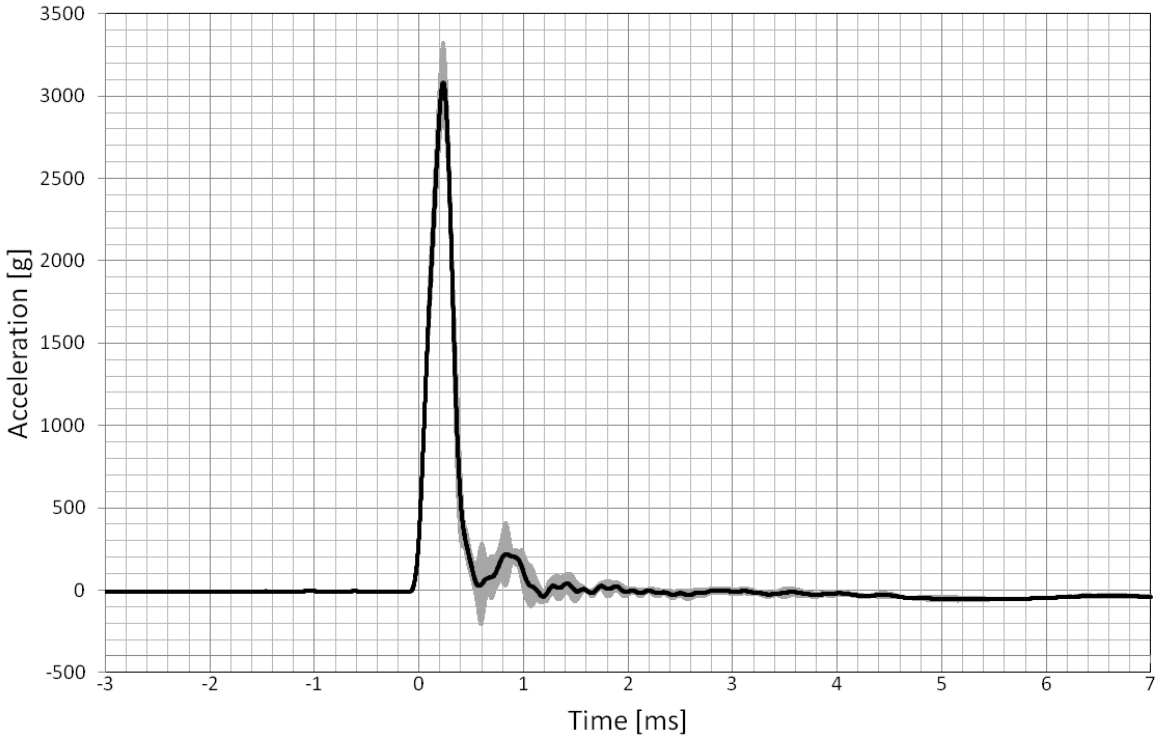

Figure 24. Shock pulse of 3000 g over 0.3 ms imparted to all sides of the bone vibrator, the average of the six pulses is shown in bold and the deviation from the average is shown in gray.

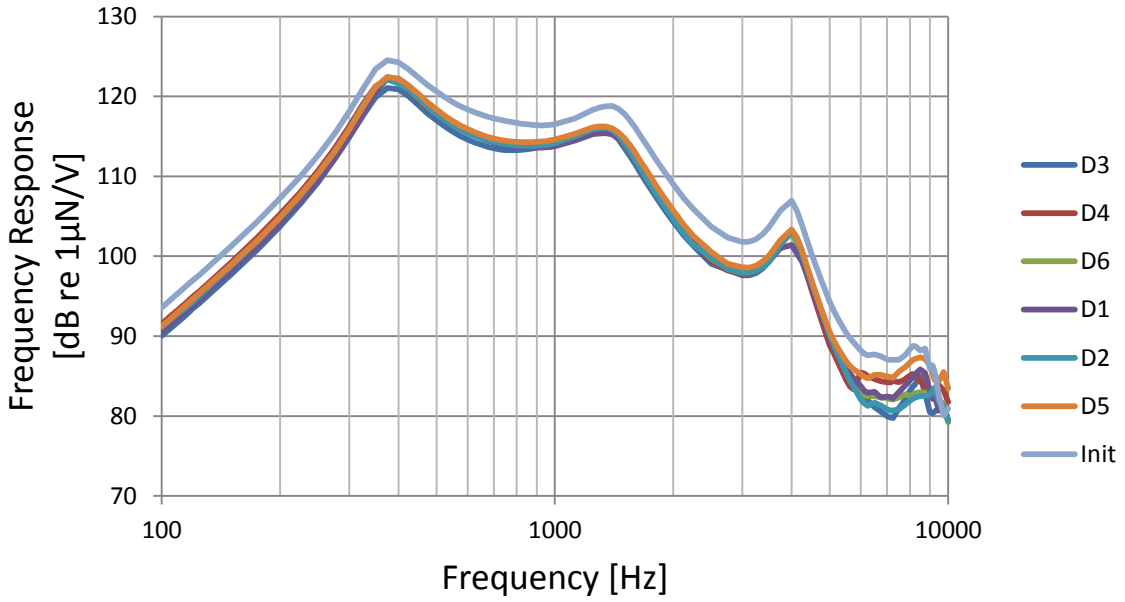

Figure 25. Frequency response of the bone vibrator after being subjected to a shock of 3000 g over the duration of 0.3 ms on all side. Init on the legend indicate frequency response before shock.

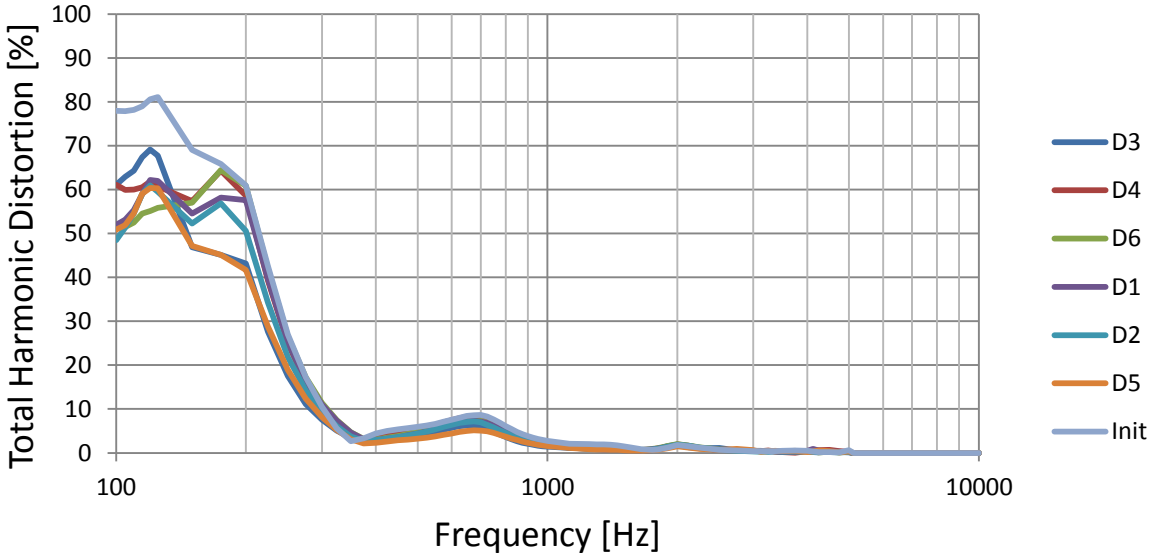

Figure 26. THD of the bone vibrator after being subjected to a shock of 3000 g over the duration of 0.3 ms on all sides. Init on the legend indicate the THD before shock.

The height needed to attain a certain peak acceleration level over a given duration using the constructed drop-test equipment was significantly less than the height calculated from equation (12). This can be due to friction at the pendulum hinge or the strike surface characteristics that the equation fails to consider (Seungbae Park, Chirag Shah, Jae Kwak, 2007).

The use of one bone vibrator for a repetitive shock is not enough to give full information about which side of the vibrator is more sensitive to the a given shock. In this regard, future work in this subject may include electro-acoustic performance investigation on larger sample size. And also it would be interesting to modify the drop-test setup to give the intended shock levels at or close to the theoretical height, calculated using equation (12). This may be done by introducing correction coefficients in the equation to account for the friction in the system and strike surface characteristics.

5. Conclusion

Drop-testing is performed to simulate the accidental drops that may occur during handling or clinical use. The design of a drop-test set up for bone vibratos and the electro-acoustic performance of one B71 bone vibrator after being subjected to varying shock severity, replicating drops, were discussed in this thesis. The designed drop-test set up was a pendulum built with an aluminum rod capable of exerting drop shocks of a half-sine waveform.

In summary:

- Vibrations from the pendulum are important to filter mechanically so that only the intended pulse is applied.
- The frequency response magnitude of B71 bone vibrator subjected to repetitive shocks starts declining from a shock level of 1500 g over 0.5 ms.
- After total exposure i.e. 1500, 2000 and 3000 g in all six directions, there was an average loss of 5.2 dB in the frequency response and 4.7 % decrease in THD.

The results indicate that the effect of applying repetitive shocks to Radioear B71 is mainly reduced gain in the frequency response of the device.

6. References

Boris Asdanin (2009), *Optimizing Mobile Phone Free Fall Drop-test Equipment – Precision, Repeatability, and Time Efficiency*, LIU-IDA/LITH-EX-A--08/060—SE.

Eeg-Olofsson M, Håkansson B Reinfeldt S, Taghavi H, Lund H, Fredén Jansson KJ, Håkansson E and Salfors J. (2014) The Bone Conduction Implant - First Implantation, Surgical and Audiologic Aspects, *Otol Neurotol*, published ahead of print.

Fredén Jansson KJ, Håkansson B, Johannsen L and Tengstrand T (2014), *The Electro-Acaustic Performance of the New Bone vibretor Radioear B81*, Submitted to International Journal of Audiology (2014).

Harpreet S. Dhiman, Xuejun Fan, Tiao Zhou (2009*), JEDEC board drop-test simulation for wafer level packages (WLPs)*, Electronic Components and Technology conference 26-29 May 2009 , San Diego, CA, pp 556 – 564.

Hearing Loss Association of America (2005), http://www.hearingloss.org/ retrieved 04 Feb 2014.

Håkansson, B. (2003), *The balanced electromagnetic separation transducer: A new bone conduction transducer, JASA*, 113(2), pp 818–825.

IEC 60318-1.*Electroacoustics - Simulators of human head and ear - Part 1: Ear simulator for the measurement of supra-aural and circumaural earphones*. Geneva :IEC ;2009 -08.

IEC 60318-3. *Electroacoustics - Simulators of human head and ear - Part 3: Acoustic coupler for the calibration of supra-aural earphones used in audiometry*. Geneva :IEC ;1998 -08.

IEC 60645-1. *Electroacoustics - Audiometric equipment - Part 1: Equipment for pure-tone audiometry.Geneva* :IEC ;2012 -02.

IEC 60068-2-27. *Environmental testing. Test methods. Environmental testing procedures. Tests. Test Ea and guidance. Shock*. Geneva :IEC ;1987.

ISO. 389-3. *Acoustics – Reference zero for the calibration of audiometric equipment – Part 3: Reference equivalent threshold force levels for pure tones and bone vibrators*. Geneva: ISO; 1994-10-01.

Seungbae Park, Chirag Shah, Jae Kwak (2007), *Transient Dynamic Simulation and Full-Field Test Validation for A Slim-PCB of Mobile Phone under Drop / Impact*. Electronic Components and Technology conference. May 29 2007-Jun 1 2007, Reno NV, pp 914-923.

Suresh Goyal ,Edward K. Buratynski (2000), *Methods for Realistic Drop-Testing*, The International Journal of Microcircuits and Electronic Packaging, Volume 23, Number1, First Quarter 2000 (ISSN 1063-1674).

Tjellström A, Håkansson B and Granström G (2001). "The bone anchored hearing aids: Current status in adults and children", *Otolaryngol. Clin. North Am.* 34(2), 337-364.

T. T. Mattila, L. Vajavaara, and J. Hokka (2013), *Evaluation of the Drop Response of Handheld Electronic Products*. Microelectronics Reliability 54(2014), pp 601-609.